Crossover Induced by Spin-Density-Wave Interference in the Coherence of Singlet Electron Pairs in Cr

J. W. A. Robinson,* Gábor B. Halász, and M. G. Blamire
Department of Materials Science and Metallurgy, University of Cambridge, Cambridge, Pembroke Street, CB2 3QZ, United Kingdom
(Received 4 June 2009; published 13 November 2009)

To study the interaction of s-wave superconductivity with spin-density waves (SDWs), we have measured a series of Nb/Cr/Nb Josephson junctions and determined the coherence length ξ describing the decay of the critical current with Cr thickness, L. We observe a crossover in ξ from approximately 14 nm to 4 nm as L increases to 10 nm, which is consistent with a transition from commensurate to incommensurate SDWs expected for this thickness range.

DOI: 10.1103/PhysRevLett.103.207002 PACS numbers: 85.25.Cp, 75.50.Ee, 75.30.Fv

The existence of ground states with multiple coexisting broken symmetries has intrigued physicists and mathematicians for decades. The coexistence of superconducting and magnetic electron correlations has now become one of the classic situations in which a ground state with more than one broken symmetry is studied, often in the form of s-wave superconductors (S) juxtaposed with ferromagnets (F) [1,2], in the heavy fermion and unconventional superconducting compounds [3], and in the layered organic superconductors [4]. A much less well understood combination of broken symmetries happens when spin-density waves (SDWs), charge density waves (CDWs), or antiferromagnetism (AFM) coexist with a superconducting ground state [5].

In all of the material systems with CDWs or SDWs and superconductors, a nexus of complex chemistry with competing ground states has made interpretation difficult. Over the years, a number of theories have proposed a simplified scheme to observe the interference effects between singlet electron pairs (SEPs) and CDWs—namely, the situation in which a Josephson junction contains a barrier with CDWs [6,7]. However, little theory has been devoted to understanding the effects of AFM and SDWs on Josephson coupling. In fact, it is generally assumed that electron-pair coherence is fairly rigid within AFM Josephson junctions resulting in long SEP decoherence times [1]; in the work reported in this Letter, we assess the coupling between SDWs and SEPs by introducing the classic itinerant antiferromagnet Cr [8] into a Nb wire to form a Nb/Cr/Nb junction. We vary the Cr thickness (L) between 1 and 20 nm. This approach has proved crucial in rapidly advancing our knowledge of the Fulde-Ferrell-Larkin-Ovchinnikov state in S-F-S junctions. Unlike in the only other existing experiment in which Josephson coupling is achieved across an antiferromagnet (γ-FeMn [9]), we observe a strong Cr-thickness-dependent SEP coherence.

Nb/Cr/Nb films were prepared on unheated 5 mm $\times$ 10 mm single crystal silicon substrates with a 250 nm thermal oxide layer on the surface. Films were deposited by dc magnetron sputtering at 1.5 Pa in Ar. The deposition chamber was baked for $\approx$7 h. Subsequently, the chamber walls were cooled with liquid nitrogen giving a base pressure of $\leq 3 \times 10^{-8}$ Pa, as confirmed by an *in situ* residual gas analyzer. Substrates were placed on a computer operated circular sample table that was mounted below stationary Nb and Cr targets. The Nb and Cr thicknesses were controlled by setting the angular speed at which the substrates moved in turn under the respective targets and by the electrical power supplied. When depositing the Cr, an acceleration curve was programmed which allowed the angular speed of the substrates to change as they passed under the Cr target so that L was dependent on the substrate position, Ω, on the rotating sample table. The rotation was programmed such that $dL/d\Omega$ was a constant. A detailed description of this wedge-growth technique can be found elsewhere [10]. Nominal film thicknesses when a substrate made a single pass at 1 rpm below the Nb and Cr targets were 5.5 nm with a power of 60 W for Nb and 0.7 nm with a power of 25 W for Cr. The angular speed variation for the Cr deposition was 0.04–1.0 rpm, which gave a set of Nb/Cr/Nb films with L linearly varying from $\approx$1 to $\approx$20 nm. The top and bottom Nb layers were 300 nm thick.

Films were etched into a series of 4 μm wide tracks using a multistep process involving optical lithography and Ar-ion milling. Each track was connected to four leads, each terminating with a large area contact pad, to allow four point measurements to be performed. In the final processing step, a focused Ga-ion beam microscope was used to form a number of current-perpendicular-to-plane devices with cross sectional areas in the $\approx(0.25$–$25) \times 10^{-14}$ mm^2 range. The complete processing technique is described in detail elsewhere [11]. Following these steps, samples were mounted onto a copper carrier and electrically connected to it with Al wires from the contact pads. The carrier was then inserted into a shielded liquid helium dip probe fitted with a solenoid, a temperature sensor, and a GHz range microwave antenna.

The current and voltage characteristics of the devices were measured using a lock-in amplifier in which the differential resistance (dV/dI) was measured as a function of bias current (I). We extract from these measurements the critical current (I_c) from the peak in the differential resistance with a well-defined noise-induced error. The normal state resistance (R_N) is measured at high bias and with a similar well-defined noise error. In Fig. 1(a), dV/dI as a function of I for two junctions with different Cr barrier thicknesses (see labels) are given with corresponding I-V curves in the figure's inset. The current and voltage of the devices followed the resistively shunted junction (RSJ) model. Because the device areas (A) vary, I_c is multiplied by R_N to give the characteristic voltage.

When irradiated with microwaves, Shapiro steps appeared in the I-V curves at integer values of $V/\varphi_0 f$, where f is the applied microwave frequency and φ_0 the flux quantum (2.067×10^{-15} Wb). These Shapiro steps are easier to observe in a plot of dV/dI versus $V/\varphi_0 f$ [see Fig. 1(b)]. In more than 80% of the I-V curves of all of the junctions measured, small Shapiro steps appeared at half-integer values of $V/\varphi_0 f$. In S-F-S π junctions, Shapiro steps at half-integer values of $V/\varphi_0 f$ have been observed at the minimum energy point of a 0 to π transition [12] and are understood to be due to a dominant second harmonic contribution to the current-phase relation of a junction's critical current [13]. They are also predicted to occur in S-F-S ϕ junctions which contain a noncentrosymmetric ferromagnet such as MnSi, for example [14]. In these junctions, microwaves are predicted to excite a precessional magnetic moment in the F layer which then interferes with the Josephson frequency of the junction resulting in half-integer Shapiro steps. The same physical explanation for the appearance of Shapiro steps at half-integer values $V/\varphi_0 f$ in Nb/Cr/Nb junctions as ϕ junctions seems unlikely; however, the addition of higher harmonic terms in the current-phase relation of a Nb/Cr/Nb junction may be reasonable. Calculations based on the Frenkel-Kontorova model [15] do predict a large second harmonic contribution to the current-phase relation of a Josephson junction when other periodic forces like SDWs interfere with the SEPs. A number of our junctions also exhibited an anomalously asymmetric dV/dI amplitude when irradiated with microwaves [see the inset of Fig. 1(b) which shows dV/dI as a function of I].

The quality of the junctions was investigated by measuring the dependence of I_c on external magnetic flux (φ) applied parallel to the Nb/Cr interfaces. Devices exhibited a Fraunhofer-shaped modulation of I_c with reentrance I_c at integer values of φ/φ_0, thus demonstrating homogeneous barriers with uniform Josephson coupling. Data from a number of devices with different Cr barrier thicknesses are given in Figs. 1(c)–1(f) with the standard Fraunhofer-like relation $I_c(\varphi) = I_c(0)\sin(\pi\varphi/\varphi_0)(\pi\varphi/\varphi_0)^{-1}$ superimposed.

In Fig. 1(g), we plot the mean values of AR_N against L. Vertical error bars represent the standard deviation of the various junctions measured for each thickness and are dominated by measurement uncertainty in the junction

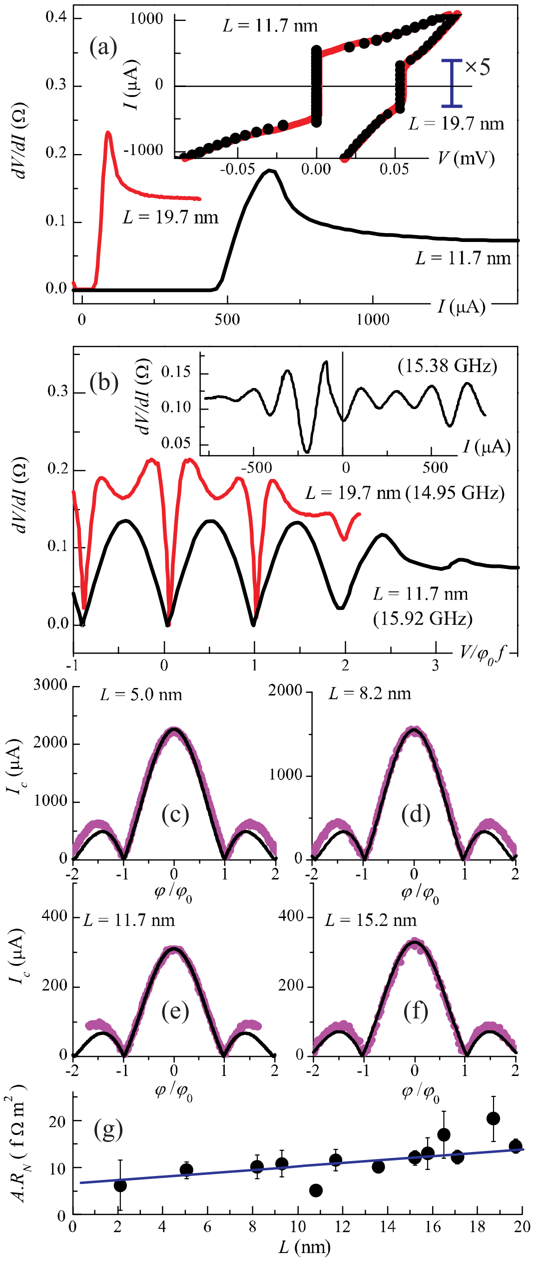

FIG. 1 (color online). (a) The differential resistance of two different junctions versus bias current at 4.2 K with their corresponding I-V curves (inset) superimposed with RSJ fits (●). The $L = 19.7$ nm data are offset from 0 voltage for clarity. (b) Effect of microwaves on the differential resistance of the same junctions in (a) plotted against $V/\varphi_0 f$. Inset: asymmetric amplitude in the differential resistance of a junction versus bias current with microwaves applied. (c)–(f) Effect of external magnetic flux on the critical current. Standard Fraunhofer-like functions are superimposed. (g) The average specific resistance of many junctions at 4.2 K versus Cr barrier thickness with a linear least-squares fit.

area. The total specific resistance in the superconducting state originates from the specific resistances of two Nb/Cr interfaces ($2AR_{\mathrm{Nb/Cr}} = 2\gamma$) and the specific resistance of the Cr barrier (ρL) such that $AR_N \approx 2\gamma + \rho L$. The gradient of the least-squares linear fit to the data in Fig. 1(g) thus provides an estimate of the average Cr resistivity $\rho = (3.6 \pm 1.5) \times 10^{-7}\ \Omega$m.

In Fig. 2, we plotted the mean I_cR_N values measured as a function of Cr barrier thickness L. Vertical error bars represent the standard deviation of the various junctions measured for each thickness and a small noise contribution from the current and voltage measurements. It is observed that I_cR_N decays with a complex dependence on L: the decay envelope is over two Cr thickness regimes separated by a crossover. In the lower thickness part, $0 < L < 8$ nm, I_cR_N is very large. For some junctions, I_c at 4.2 K was extrapolated from higher temperature data. To make this extrapolation, a phenomenological relationship between I_c and T was determined by measuring the thermal dependence of I_c in other junctions in which I_c could be measured at 4.2 K. We found that I_c was well described by the phenomenological relation $I_c(\mathrm{T}) = I_c(0)[1 - (T/T_c)^2]$, where $I_c(0)$ is the critical current at 0 K and T_c the superconducting transition temperature of Nb. Typical $I_c(T)$ data are given in the inset of Fig. 2. In the Cr thickness range $8 < L < 12$ nm, I_cR_N drops by an order of magnitude, signaling a change in the decoherence time of the SEPs.

At the largest Cr barrier thicknesses used in these experiments, the data tend to an exponential decay with an effective coherence length of ≈ 4 nm. No simple theory exists to calculate I_cR_N of an artificial Josephson junction with SDWs in the barrier. A good starting point is to apply

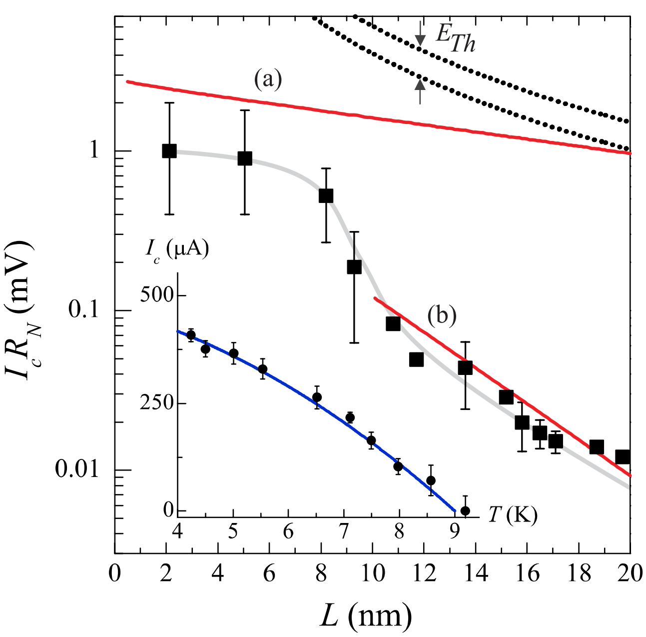

FIG. 2 (color online). The decay in the average characteristic voltage of many devices as a function of Cr barrier thickness (L) at 4.2 K ($L > 8.0$ nm) and extrapolated from higher temperature data ($L < 8.0$ nm) as explained in the main text. All I_cR_N values fall below the Thouless energy E_{Th}. Curves labeled a and b are described within the main text. Inset: the typical thermal dependence of a junction's critical current (I_c) with a phenomenological fit superimposed, as described in the main text.

the Usadel equation which is often used to describe the properties of diffusive S-N-S (N stands for normal metal) junctions with arbitrary scattering [1]. In solving the Usadel equation, the characteristic voltage can be shown to be

$$eI_cR_N = \pi k_B T L_0 \sum_{\omega>0} \frac{\Delta^2}{\hbar^2\omega^2} \frac{2k/\cosh(kL)}{\tanh(kL)(1 + k^2\Gamma^2) + 2k\Gamma}, \tag{1}$$

where $L_0 = L + 2\gamma/\rho$, $k = \xi^{-1} = (2\omega/D)^{-1/2}$, and $\Gamma = \gamma\sqrt{\Delta^2 + \hbar^2\omega^2}/\hbar\rho\omega$. The summation goes over the positive Matsubara frequencies $\omega = (2m + 1)\pi k_B T/\hbar$, where m is an integer number. The magnitude of the pairing potential (Δ) is assumed to be constant and identical in both superconducting leads with its value determined from

$$\ln\frac{T_c}{T} = 2\pi k_B T \sum_{\omega>0}\left(\frac{1}{\hbar\omega} - \frac{1}{\sqrt{\Delta^2 + \hbar^2\omega^2}}\right). \tag{2}$$

From the calculated value of the Cr resistivity, we can determine the electron mean free path (l) and the electron diffusivity (D) in the Cr barrier, which are needed to apply the above model. From the relation $l = m_e v_F/N\rho e^2$, where m_e is the electron mass, e the electron charge, and N_d the number density of electrons, $l \approx 1.2 \pm 0.3$ nm if we assume a typical Fermi velocity (v_F) of 2×10^6 ms^{-1} for a transition metal. The average electron diffusivity is thus $D = v_F l/3 \approx 7.7 \pm 1.5 \times 10^{-4}$ m^{2}s^{-1} and hence demonstrates that all I_cR_N values measured in our experiment fall below the Thouless energy $E_{\mathrm{Th}} = \hbar D/eL^2$ (in volts). These results imply short junction behavior in the Cr barrier with transport across the Nb/Cr interfaces dominated by Δ [16] (see dotted curves in Fig. 2).

Applying these material parameters to Eqs. (1) and (2) results in a slow decay in I_cR_N with an electron-pair coherence length in Cr of $\xi \approx 14$ nm (see curve a in Fig. 2). This is clearly inconsistent with the $L > 12$ nm data and thus implies a modified scattering relaxation time in this higher thickness regime. For S-N-S junctions, this relaxation time (τ) modifies ω to $\omega \rightarrow \omega + \tau^{-1}$ and is often used as a phenomenological parameter to express the effects of additional pair-breaking processes [1]. In Fig. 2, we plot the best fit, labeled b, to the $L > 12$ nm data, which yields a relaxation time of $\approx 4 \times 10^{-14}$ s and a coherence length of $\xi = \sqrt{D\tau/2} \approx 4$ nm, which is more consistent with the experimental results.

Detailed Mössbauer spectroscopy experiments on Cr/V multilayers report the stabilization of commensurate SDWs (C-SDW) around $L = 3.0$ nm while the nonmagnetic interface is only ≈ 2 Å [17]. Other experiments with Cr [18] and Cr/F [19] multilayers also suggest that above $L = 3$–6 nm, the SDWs undertake a transformation from C- to incommensurate- (I-) SDW phases due to strain relaxation and fewer impurities. Our low thickness results are consistent with this picture since for a commensurate

C-SDW (i.e., simple AFM [1]) the antiferromagnetic exchange field averages to zero and so the coherence length is given by $\xi = \sqrt{\hbar D/2\pi k_B T}$ [1], i.e., 14 nm for our structure. We consequently infer that the enhanced decoherence at higher thicknesses is associated with scattering from I-SDWs.

Finally, band structure calculations [20] and neutron diffraction studies of single crystal Cr with dilute (2%) Mn impurities [21] suggest that Cr spin waves have an associated velocity of the order 3×10^5 ms^{-1}. In our Cr, the crossover thickness 8–12 nm provides an estimate for the wavelength, λ, of a SDW and so it is plausible that the product $\lambda\tau^{-1}$ should be physically related to an effective spin-wave velocity which is also of the order 10^5 ms^{-1}.

This Letter has shown that, in agreement with predictions, Josephson coupling across a simple AFM metal occurs with minimal additional decoherence compared to a simple metal. However, our experiment suggests that the nucleation of incommensurate spin-density waves results in a severely reduced electron-pair decoherence time and thus in a suppressed Josephson critical current. The precise scattering mechanism is currently not known or understood and so requires the development of a new first-principles theory.

This work was supported by UK Engineering and Physical Sciences Research Council (Grants No. EP/F016611 and No. EP/E026206). J. W. A. R. was supported by St. John's College, Cambridge. The authors acknowledge Dr. K. Sandeman (Imperial College, UK) for insightful discussions and G. B. H. wishes to thank Professor J. Driscoll, Trinity College, Cambridge for supporting this work.

Note added in proof.—Recently, Weides *et al.* submitted interesting results to Physical Review B on the topic of Nb/AlO_x/Cr/Nb Josephson tunnel junctions [22].

*jjr33@cam.ac.uk

[1] A. I. Buzdin, Rev. Mod. Phys. **77**, 935 (2005).
[2] F. S. Bergeret, A. F. Volkov, and K. B. Efetov, Rev. Mod. Phys. **77**, 1321 (2005).
[3] D. Aoki *et al.*, Nature (London) **413**, 613 (2001); T. Park *et al.*, Nature (London) **440**, 65 (2006).
[4] S. Lefebvre *et al.*, Phys. Rev. Lett. **85**, 5420 (2000).
[5] A. M. Gabovich *et al.*, Supercond. Sci. Technol. **14**, R1 (2001).
[6] M. I. Visscher and B. Rejaei, Phys. Rev. Lett. **79**, 4461 (1997).
[7] S. Duhot and R. Mélin, Eur. Phys. J. B **55**, 289 (2007).
[8] E. Fawcett, Rev. Mod. Phys. **60**, 209 (1988); E. Fawcett *et al.*, *ibid.* **66**, 25 (1994).
[9] C. Bell *et al.*, Phys. Rev. B **68**, 144517 (2003).
[10] J. W. A. Robinson *et al.*, Phys. Rev. Lett. **97**, 177003 (2006).
[11] C. Bell *et al.*, Nanotechnology **14**, 630 (2003).
[12] H. Sellier *et al.*, Phys. Rev. Lett. **92**, 257005 (2004).
[13] A. Buzdin, Phys. Rev. B **72**, 100501 (2005).
[14] F. Konschelle and A. Buzdin, Phys. Rev. Lett. **102**, 017001 (2009).
[15] B. Hu and J. Tekić, Phys. Rev. E **75**, 056608 (2007).
[16] J. K. Freericks *et al.*, IEEE Trans. Appl. Supercond. **15**, 896 (2005).
[17] M. Almokhtar *et al.*, J. Phys. Condens. Matter **12**, 9247 (2000).
[18] M. Takeda *et al.*, Phys. Rev. B **70**, 104408 (2004); E. Rotenberg *et al.*, New J. Phys. **7**, 114 (2005); Z. Boekelheide, E. Helgren, and F. Hellman, Phys. Rev. B **76**, 224429 (2007).
[19] A. Schreyer *et al.*, Phys. Rev. Lett. **79**, 4914 (1997); I. A. Garifullin *et al.*, Phys. Rev. B **70**, 054505 (2004); J. S. Parker *et al.*, Phys. Rev. Lett. **97**, 227206 (2006).
[20] R. P. Gupta and S. K. Sinha, Phys. Rev. B **3**, 2401 (1971).
[21] S. K. Sinha *et al.*, Phys. Rev. Lett. **23**, 311 (1969).
[22] M. Weides *et al.*, Phys. Rev. B **80**, 064508 (2009).